# Beneficial effects of cordycepin on metabolic profiles of liver and plasma from hyperlipidemic hamsters

Yang Sun [a] , Ying-Hong Wang [a] , Kai Qu [a] & Hai-Bo Zhu [a]

[a] Key Laboratory of Bioactive Substances and Resources Utilization
of Chinese Herbal Medicine, Ministry of Education and Key
Laboratory of Natural Drugs Biosynthesis, Ministry of Health,
Institute of Materia Medica, Chinese Academy of Medical Sciences
and Peking Union Medical College, Beijing, 100050, China

Available online: 25 May 2011

PLEASE SCROLL DOWN FOR ARTICLE

Taylor & Francis
Taylor & Francis Group

# Beneficial effects of cordycepin on metabolic profiles of liver and plasma from hyperlipidemic hamsters

Yang Sun, Ying-Hong Wang, Kai Qu and Hai-Bo Zhu*

*Key Laboratory of Bioactive Substances and Resources Utilization of Chinese Herbal Medicine, Ministry of Education and Key Laboratory of Natural Drugs Biosynthesis, Ministry of Health, Institute of Materia Medica, Chinese Academy of Medical Sciences and Peking Union Medical College, Beijing 100050, China*

In this study, $^1$H NMR-based metabonomics was applied to evaluate the beneficial effects of cordycepin (3′-deoxyadenosine), a natural monomer compound, on endogenous metabolic profiles of liver and plasma from hyperlipidemic Syrian golden hamsters. Hyperlipidemia was successfully established in hamsters fed by a high-fat diet for 2 weeks. The hyperlipidemic hamsters were treated with an oral administration of simvastatin ($2\,mg\,kg^{-1}$) or cordycepin ($140\,mg\,kg^{-1}$) for consecutive 4 weeks. The metabolic profiles of plasma and intact liver tissues were established using $^1$H NMR spectroscopy. The results showed higher contents of lipids (triglyceride and cholesterol), lactate, acetate, alanine, glutamine together with lower contents of choline-containing compounds (e.g. phosphocholine, phosphatidylcholine, and glycerophosphocholine), glucose, and glycogen in plasma and liver samples from hyperlipidemic hamsters than those in controls. Cordycepin afforded a little lipid-regulating activity on plasma but more beneficial effects on liver, implicating that cordycepin might have a protective effect on liver under fatty liver condition.

**Keywords:** hyperlipidemia; nuclear magnetic resonance (NMR) spectroscopy; metabonomics; hyperlipidemic hamsters; cordycepin

## 1. Introduction

Hyperlipidemia, the prevalence of which is increasing rapidly worldwide, is a major cause of atherosclerosis and atherosclerosis-associated conditions, such as coronary heart disease, ischemic cerebrovascular disease, and peripheral vascular disease.

Antidyslipidemic drugs that are currently used in clinical treatment include statins – HMG–CoA inhibitors, fibrates, niacin, ezetimibe, and bile acid sequestrants, among which statins are the most effective and widely used drugs [1].

An increasing number of patients treated with statins suffer from its side effects (e.g. the incidence of hepatotoxicity and myopathy). Thus, additional pharmaceutical strategies are required to resolve problems in efficacy and tolerability of hyperlipidemia [1], and the development and use of novel effective hypolipidemic agents remain of crucial importance.

Cordycepin, highly structurally analogous to adenosine (Figure 1), also known as 3′-deoxyadenosine, is a bioactive compound present in the species of fungi belonging to the genus Cordyceps used as a tonic herb in traditional Chinese medicine, which possesses antihyperlipidemic activity in our previous *in vivo* and *in vitro* experiments. In recent years, many pharmacological properties of cordycepin

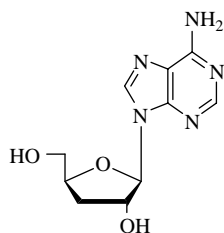*Corresponding author. Email: zhuhaibo@imm.ac.cn

Figure 1. Structure of cordycepin.

have been uncovered, including anti-virus, anti-fungus, anti-inflammation, anti-hyperglycemia [2] and anti-atherosclerosis. In the previous study, we investigated the antihyperlipidemic capacities of cordycepin in Syrian golden hamsters that fed a high-fat diet (HFD) in which the lipid-lowering effect afforded by adenosine-like compound to date was discovered for the first time [3].

Studies in hypolipidemic drugs are mainly based on serum or plasma biochemical examination and histopathological evaluation. However, nontargeted metabonomics technologies have the potential for providing novel biomarkers of disease and drug efficacy [4]. Metabonomics technologies are currently experiencing an exponential increase in their incorporation into biological studies with applications ranging from physiological genomics and potential lead target validation [5,6] through mechanistic toxicology [7] to clinical pharmacology [8], disease investigation [9,10], and so on.

Nuclear magnetic resonance (NMR) spectroscopy-based metabonomics could provide a comprehensive picture of metabolic changes induced by studying drugs. In this study, NMR-based metabonomics was used to evaluate whether the beneficial effects of cordycepin exist in hyperlipidemic hamsters.

## 2. Results and discussion

### 2.1 Metabolites identification

Metabolites identified in plasma and liver samples are shown in Table 1.

### 2.2 Metabolite changes observed by NMR-based metabonomics

Initial visual inspection of the data showed higher concentrations of lipids, lactate together with lower concentrations of choline-containing compounds, and glucose in plasma and liver samples from hyperlipidemic hamsters than those in controls. However, the treatment of simvastatin or cordycepin made changes in the reverse direction (Figure 2). Further investigation of the metabolic consequences of the disease was performed using pattern recognition (PR) techniques.

### 2.3 Metabolite changes in plasma

Principal component analysis (PCA) scores and loadings plot of the $^1$H BPP-LED NMR spectral data of plasma samples showed an apparent higher level of low-density lipoprotein/very low-density lipoprotein (LDL/VLDL) ($\delta$ 0.9, 1.30), $N$-acetyl glycoproteins ($N$-Ac, $\delta$ 2.04), and some of the lipid signals including $CH_2$—$CH_2CO$ ($\delta$ 1.58), $CH_2$—$CH =$ ($\delta$ 2.02), $CH$═$CH$ ($\delta$ 5.34), $CH_2$—$CO$ ($\delta$ 2.26), accompanied with the lower level of high-density lipoprotein (HDL) ($\delta$ 0.86, 1.26), phosphatidyl-choline (PtdCho) ($\delta$ 3.22) in the plasma samples of hyperlipidemic hamsters than those in controls (Figure 3(A), (B) and Table 2).

There was a decrease in lipid signals (e.g. LDL/VLDL) in the plasma of hyperlipidemic hamsters after 4-week treatment with simvastatin or cordycepin, suggesting that both simvastatin and cordycepin made an improvement on plasma lipid metabolites caused by hyperlipidemia (Figure 3(C)).

OPLS-DA analysis identified the metabolic changes of plasma samples observed in $^1$H CPMG-NMR spectra of control and hyperlipidemic hamsters (Figure 4(A)), including an increase in the signal intensities of lactate ($\delta$ 1.34), alanine ($\delta$ 1.46), acetate ($\delta$ 1.94), glutamine ($\delta$ 2.14, 2.46), and little lipid

Table 1.  [1]H chemical shift assignment of the metabolites of plasma and liver from hamsters.

| Biological matrices | Metabolites | Moieties | $\delta^1$H(ppm) and multiplicity |
|---|---|---|---|
| Plasma | Leucine | $\gamma CH_3$ | 0.95 (d) |
| | Valine | $\gamma CH_3, \gamma' CH_3$ | 0.98 (d), 1.03 (d) |
| | Isoleucine | $\delta CH_3$ | 1.01 (d) |
| | 3-HB | $\gamma CH_3$ | 1.20 (d) |
| | Lactate | $\beta CH_3, \alpha CH$ | 1.34 (d), 4.11 (q) |
| | Lysine | $\gamma CH_2$ | 1.45 (m) |
| | Alanine | $\beta CH_3$ | 1.46 (d) |
| | Acetate | $\beta CH_3$ | 1.94 (s) |
| | *N*-acetyl glycoproteins | $CH_3$ | 2.04 (s) |
| | *O*-acetyl glycoproteins | $CH_3$ | 2.06 (s) |
| | Methionine | $S{-}CH_3$ | 2.13 (s) |
| | Acetoacetate | $CH_3$ | 2.29 (s) |
| | Pyruvate | $CH_3$ | 2.41 (s) |
| | Glutamine | $\gamma CH_2$ | 2.14 (m), 2.46 (m) |
| | Creatine | $N{-}CH_3$ | 3.03 (s) |
| | Betaine | $N(CH_3)_3$ | 3.26 (s) |
| | Taurine | $N{-}CH_2, S{-}CH_2$ | 3.24 (t), 3.42 (t) |
| | TMAO | $N(CH_3)_3$ | 3.26 (s) |
| | Tyrosine | CH,CH | 6.87 (m), 7.16 (m) |
| | Choline | $N(CH_3)_3$ | 3.20 (s) |
| | Phosphocholine/GPC | $N(CH_3)_3$ | 3.22 (s) |
| | Phosphatidylcholine | $N(CH_3)_3$ | 3.22 (s) |
| | $\alpha$-Glucose | CH | 5.22 (d) |
| | $\beta$-Glucose | CH | 4.62 (d) |
| | Glucose/amino acids resonances | Ring protons/$\alpha$-CH | 3.4–4.0 |
| | Lipids (VLDL/LDL) | $-CH_3$ | 0.9 (t) |
| | Lipids (VLDL/LDL) | $-(CH_2)_n-$ | 1.30 (m) |
| | Lipids (HDL) | $-CH_3$ | 0.86 (t) |
| | Lipids (HDL) | $-(CH_2)_n-$ | 1.26 (m) |
| | Lipids | $-CH_2CH_2CO$ | 1.61 (m) |
| | Lipids | $-CH_2CH{=}$ | 2.02 (m) |
| | Lipids | $-CH_2CO$ | 2.26 (m) |
| | Lipids | ${=}CHCH_2CH{=}$ | 2.78 (m) |
| | Unsaturated lipids | $-CH{=}CH-$ | 5.34 (m) |
| Intact liver | Leucine | $\gamma CH_3$ | 0.95 (d) |
| | Valine | $\gamma CH_3, \gamma' CH_3$ | 0.98 (d), 1.03 (d) |
| | Isoleucine | $\delta CH_3$ | 1.01 (d) |
| | 3-HB | $\gamma CH_3$ | 1.20 (d) |
| | Lactate | $\beta CH_3, \alpha CH$ | 1.34 (d), 4.11 (q) |
| Intact liver | Lysine | $\gamma CH_2$ | 1.45 (m) |
| | Alanine | $\beta CH_3$ | 1.46 (d) |
| | Acetate | $\beta CH_3$ | 1.94 (s) |
| | Glutamine | $\gamma CH_2$ | 2.14 (), 2.46 (m) |
| | Acetoacetate | $CH_3$ | 2.29 (s) |
| | Betaine | $N(CH_3)_3$ | 3.26 (s) |
| | Taurine | $N{-}CH_2, S{-}CH_2$ | 3.26 (t), 3.42 (t) |
| | TMAO | $N(CH_3)_3$ | 3.26 (s) |
| | Choline | $N(CH_3)_3$ | 3.20 (s) |
| | Phosphocholine/GPC | $N(CH_3)_3$ | 3.22 (s) |
| | $\alpha$-Glucose | CH | 5.22 (d) |
| | $\beta$-Glucose | CH | 4.62 (d) |
| | Glucose/glycogen/$\alpha$-H amino acids | Ring protons/$\alpha$-CH | 3.4–4.0 |
| | Glycogen | CH | 5.38–5.44 |

Table 1 – *continued*

| Biological matrices | Metabolites | Moieties | $\delta^1$ H(ppm) and multiplicity |
|---|---|---|---|
| | Lipids | $-CH_3$ | 0.9–0.94 (m) |
| | Lipids | $-(CH_2)_n-$ | 1.30–1.34 (m) |
| | Lipids | $-CH_2CH_2CO$ | 1.61 (m) |
| | Lipids | $-CH_2CH=$ | 2.02 (m) |
| | Lipids | $-CH_2CO$ | 2.26 (m) |
| | Lipids | $=CHCH_2CH=$ | 2.78 (m) |
| | Unsaturated lipids | $-CH=CH-$ | 5.30 (m) |

Notes: s, singlet; d, doublet; dd, double doublet; t, triplet; q, quartet; and m, multiplet.

signals ($\delta$ 0.90, 0.94, 5.30) accompanied with a reduction in betaine ($\delta$ 3.26), glycerophosphorylcholine (GPC) ($\delta$ 3.22), and glucose ($\delta$ 3.40–4.00) in hyperlipidemic hamsters (Table 2).

The modality of low-molecular-weight metabolites of the plasma in hyperlipidemic hamsters with administration of cordycepin was not better than that of simvastatin (Figure 4(B)).

### 2.4 Metabolite changes in intact liver

The results presented clear differences between the metabolic profiles of liver samples from hyperlipidemic hamsters and controls (Figure 5(A)). Livers from hyperlipidemic hamsters were associated with the increased levels of lipids (e.g. CH$_3$ ($\delta$ 0.9–0.94), (CH$_2$)$_n$ ($\delta$ 1.30–1.34), CH$_2$—CH=($\delta$ 2.02), and CH$_2$CO ($\delta$ 2.26)), lactate, alanine, acetate, glutamine, and with the decreased levels of choline-containing compounds (e.g. phosphocholine, GPC) ($\delta$ 3.22), glucose, and glycogen ($\delta$ 3.40–4.00, 5.38–5.44) (Figure 5(B) and Table 2).

However, these metabolites of hyperlipidemic hamsters treated with simvastatin or cordycepin changed in the opposite direction. Scores plot of OPLS-DA representing the four groups of hamsters indicated that cordycepin appeared to be better than simvastatin in lipid metabolic profiles of the liver (Figure 5(C)).

Comparing the metabolic profiles of liver samples obtained by $^1$H CPMG-NMR spectra of control and hyperlipidemic hamsters, the predominant changes identified in the OPLS-DA analysis included an increase in the signal intensities of lactate, alanine, acetate, glutamine, and lipid signals accompanied with a reduction in the intensities of GPC ($\delta$ 3.2–3.24), glucose, and glycogen in hyperlipidemic hamsters (Table 2). The hyperlipidemic hamsters with the treatment of cordycepin reversed this tendency, implying that cordycepin improved the liver profiles and had more beneficial effects than simvastatin on liver (Figure 6).

### 2.5 Discussion

In our study, it was revealed that cordycepin afforded not only lipid-regulating activity on the plasma but also beneficial effects on the liver tissues of hyperlipidemic hamsters by NMR-based metabonomics.

Here, the hyperlipidemic hamster model was used to investigate the effects of cordycepin, which was previously established for studying diet-induced hyperlipidemia [11,12].

Though it has been proved that cordycepin had a lipid-regulating effect on both plasma and liver in the previous study [3], NMR-based metabonomics showed a wide picture of endogenous
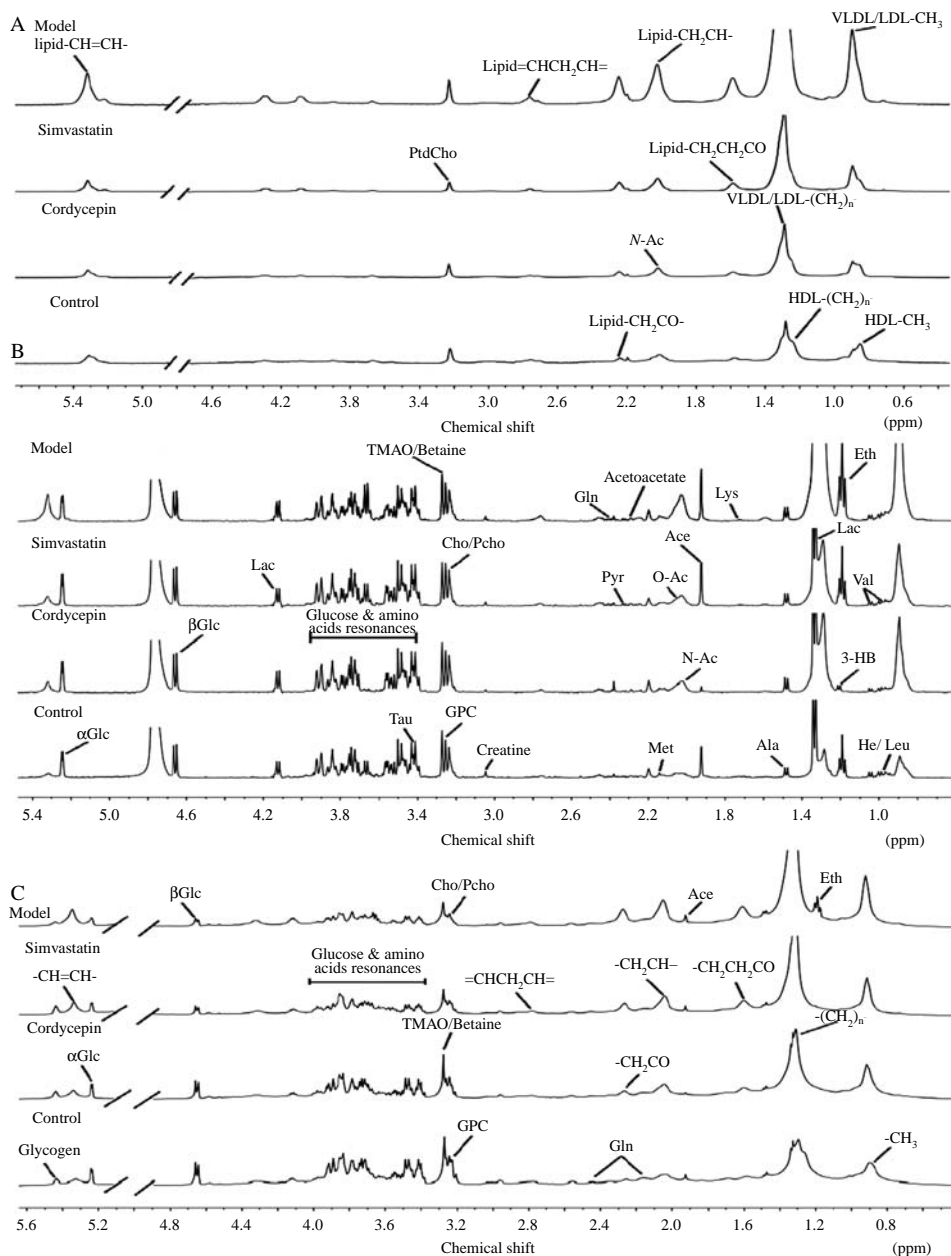
Figure 2.   Typical 500 MHz ^{1}H NMR spectra of plasma and liver samples from the four groups of hamsters. (A): ^{1}H NMR BPP-LED spectra of plasma samples. (B): ^{1}H NMR CPMG spectra of plasma samples. (C): HR-MAS ^{1}H NMR standard spectra of liver tissues. Signal assignment: VLDL, very-low-density lipoprotein; LDL, low-density lipoprotein; HDL, high-density lipoprotein; PtdCho, phosphatidylcholine; Ile, isoleucine; Leu, leucine; 3-HB, 3-D-hydroxybutyrate; Val, valine; Eth, ethanol (residual); Lac, lactate; Ala, alanine; Lys, lysine; Ace, acetate; *N*-Ac, *N*-acetyl glycoproteins; *O*-Ac, *O*-acetyl glycoproteins; Met, methionine; Pyr, pyruvate; Gln, glutamine; Cho, choline; GPC, glycerophosphorylcholine; Glc, glucose; and TMAO, trimethylamine-*N*-oxide.
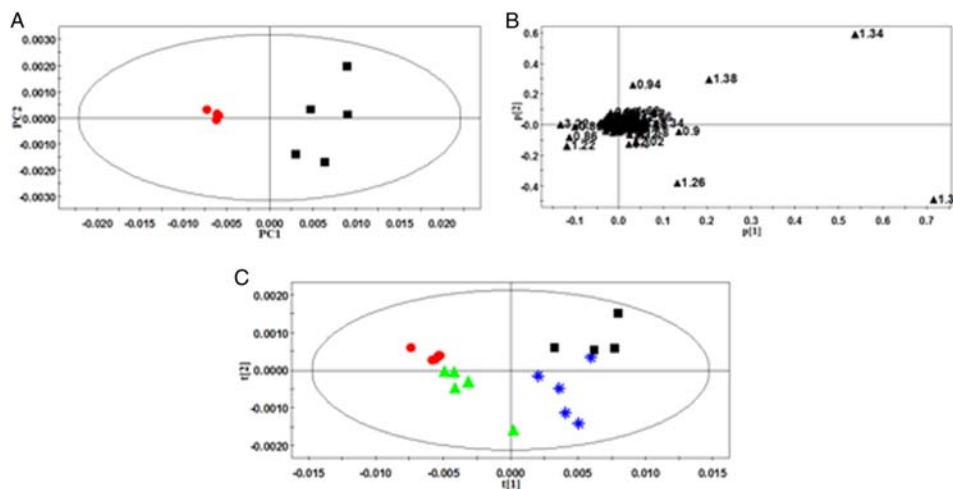
Figure 3. PR analysis of $^1$H NMR BBP-LED spectra of plasma from hamsters. (A): PCA scores plot of $^1$H NMR BBP-LED spectra of plasma from normal and hyperlipidemic hamsters. (B): Corresponding loadings plot of (A). (C): Scores plot of OPLS-DA analysis of the spectra of plasma from the four groups of hamsters. ●, Control hamsters; ■, hyperlipidemic hamsters; ▲, hyperlipidemic hamsters treated with simvastatin (2 mg kg$^{-1}$); and ∗, hyperlipidemic hamsters with administration of cordycepin (140 mg kg$^{-1}$).

metabolites such as acetate, alanine, glutamine, and betaine, which can hardly be found by the conventional pharmacological methods.

Compared with the controls, the higher concentrations of lipids (triglycerides and cholesterol), lactate, acetate, alanine, glutamine, together with the lower concentrations of choline-containing compounds (e.g. phosphocholine, PtdCho, and GPC), glucose, and glycogen, in plasma and liver samples from hyperlipidemic hamsters were observed. However, the levels of these metabolites moved toward normal when hyperlipidemic hamsters were treated with simvastatin or cordycepin.

More importantly, NMR-based metabonomics gave us highlight that cordycepin had better hypolipidemic and beneficial effects than simvastatin on liver. Simvastatin mainly had a little lipid-lowering effect and hardly made changes in low-molecular weight metabolites that perform a vital role in glucose/glycogen and lipid metabolism in liver.

The changes of macromolecules in plasma caused by cordycepin contained apparent lower levels of LDL/VLDL, *N*-Ac, and some of the lipid signals including $CH_2$—$CH_2$, CH=CH, C2, and C3 protons of fatty acids, accompanied with the higher levels of HDL and PtdCho than those in hyperlipidemic hamsters. An increase in the signal at δ 3.22 (PtdCho) observed is consistent with the higher level of HDL because PtdCho is the most predominant lipid in the HDL fraction [13–15]. The total lipid concentration in the plasma of hyperlipidemic hamsters with administration of cordycepin was lower than that in untreated hyperlipidemic hamsters, as indicated by the loadings of resonances at δ 2.26 and δ 1.58, contributed from the C2 and C3 protons of fatty acids (Figure 3(B)).

The micromolecules in the plasma of hyperlipidemic hamsters treated by cordycepin changed, including a reduction in the signals of lactate, alanine, acetate, glutamine, accompanied with an increase in taurine, betaine, GPC, and glucose. Higher

Table 2. Changes in the metabolites of plasma and liver from the groups of hamsters.

| Biological matrices | Metabolites | Hyperlipidemic hamsters[#] | Hyperlipidemic treated with WS070117[*] |
|---|---|---|---|
| Plasma | LDL/VLDL | ↑ | ↓ |
| | $N$-Ac | ↑ | ↓ |
| | $-CH_2-CH_2CO$[a] | ↑ | ↓ |
| | $-CH_2-CH=$[a] | ↑ | ↓ |
| | $-CH_2CO$[a] | ↑ | ↓ |
| | $-CH=CH$[a] | ↑ | ↓ |
| | Lactate | ↑ | ↓ |
| | Alanine | ↑ | ↓ |
| | Acetate | ↑ | ↓ |
| | Glutamine | ↑ | ↓ |
| | HDL | ↓ | ↑ |
| | PtdCho | ↓ | ↑ |
| | Betaine | ↓ | ↑ |
| | Cho/Pcho | ↓ | ↑ |
| | GPC | ↓ | ↑ |
| | Glucose | ↓ | ↑ |
| Liver | $-CH_3$[a] | ↑ | ↓ |
| | $-(CH_2)_n-$[a] | ↑ | ↓ |
| | $-CH_2-CH=$[a] | ↑ | ↓ |
| | $-CH_2CO$[a] | ↑ | ↓ |
| | Alanine | ↑ | ↓ |
| | Lactate | ↑ | ↓ |
| | Acetate | ↑ | ↓ |
| | Glutamine | ↑ | ↓ |
| | Cho/Pcho | ↓ | ↑ |
| | GPC | ↓ | ↑ |
| | Glucose/glycogen | ↓ | ↑ |

Notes: ↑, Increase in content; and ↓, decrease in content.
[#] Compared with control hamsters.
[*] Compared with hyperlipidemic hamsters.
[a] Moieties in lipid.

glucose and lower lactate and total lipid levels in hyperlipidemic hamsters administrated with cordycepin suggested that the rate of glycolysis was reduced and the energy consumption was switched to lipid oxidation. We anticipated that lactate and alanine would be depleted in the plasma, consistent with decreased gluconeogenesis through the glucose–alanine and Cori cycles. Therefore, the reduction in alanine caused by cordycepin indicated that muscle proteins degration and liver gluconeogenesis were inhibited.

There were decreased levels of lipids (e.g. $CH_3$, $(CH_2)_n$, $CH_2-CH=$, and $CH_2CO$), lactate, alanine, acetate, glutamine and increased levels of choline-containing compounds (e.g. phosphocholine and GPC), glucose, and glycogen in liver tissues from hyperlipidemic hamsters treated with cordycepin.

As VLDL synthesis requires the availability of phospholipids, particularly PtdCho, an insufficiency of PtdCho or its precursors can lead to decreased secretion of triglycerides from the liver and hence fatty liver. Cordycepin increased the levels of phospholipids (i.e. PtdCho) in hyperlipidemic hamsters, so it can promote triglycerides export from the liver to prevent fat accumulation. Cordycepin was also found to increase hepatic GPC, which may be an indicator of liver 'functionality' [16].
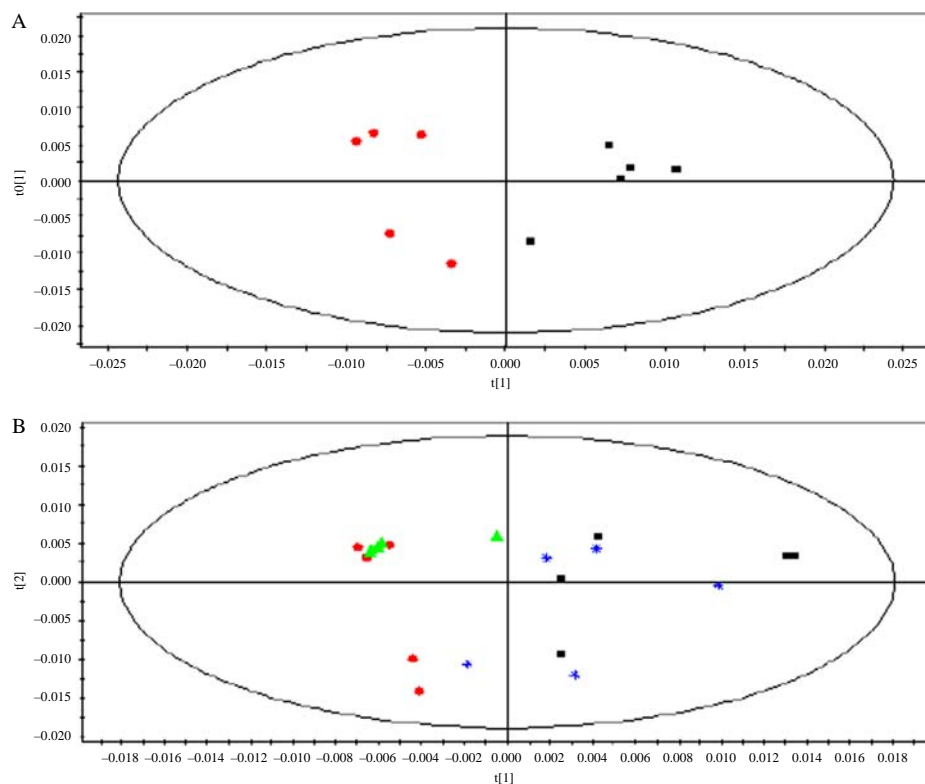
Figure 4. PR analysis of $^1$H NMR CPMG spectra of plasma from hamsters. (A): PCA of the spectra of plasma from normal and hyperlipidemic hamsters. (B): Scores plot of OPLS-DA analysis of the spectra of plasma from the four groups of hamsters. ●, Control hamsters; ■, hyperlipidemic hamsters; ▲, hyperlipidemic hamsters treated with simvastatin (2 mg kg$^{-1}$); and *, hyperlipidemic hamsters with administration of cordycepin (140 mg kg$^{-1}$).

In our research, higher levels of glucose and glycogen observed in the liver were suggestive of depleted glycolysis and glycogenolysis and may also indicate that cordycepin could decrease energy demands, indicating that AMPK may be activated [3].

Several factors may contribute to the rising acetate levels in plasma including (1) impaired mitochondrial substrate oxidation, (2) induction of acetyl-CoA synthetase 2 under ketogenic conditions, and (3) increased acetate release from the liver. Cordycepin can reduce acetate in plasma from hyperlipidemic hamsters indicating its improvement in fatty liver progress.

The HR-MAS $^1$H NMR spectrum of liver showed that the pronounced differences in hepatic lipid content and choline-containing compounds existed between hyperlipidemic golden hamsters treated and untreated with cordycepin.

These findings showed that NMR-based metabonomics did give a better picture of the multiparametric response to hyperlipidemia and pharmacological intervention with a natural compound cordycepin, which provided new clues in understanding the beneficial effects of cordycepin on endogenous metabolic profiles of liver and plasma from hyperlipidemic hamsters.

As only plasma and liver samples were studied here, further investigations with urine and biles are needed to generate a more complete mechanistic pathway for
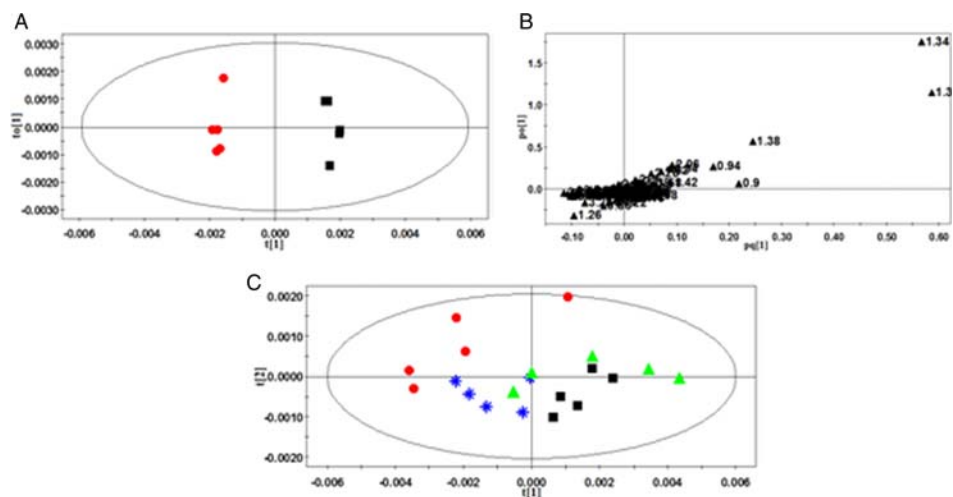
Figure 5. PR analysis of HR-MAS $^1$H NMR spectra of liver tissues from hamsters. (A): PCA scores plot of $^1$H NMR spectra of liver tissues from normal and hyperlipidemic hamsters. (B): Corresponding loadings plot of (A). (C): Scores plot of OPLS-DA analysis of the spectra of plasma from the four groups of hamsters. ●, Control hamsters; ■, hyperlipidemic hamsters; ▲, hyperlipidemic hamsters treated with simvastatin (2 mg kg$^{-1}$); and *, hyperlipidemic hamsters with administration of cordycepin (140 mg kg$^{-1}$).

understanding the hypolipidemic effect of cordycepin in our next work.

The observations demonstrated for the first time that cordycepin, a natural compound, can modify metabolites of liver and plasma from hyperlipidemic golden hamsters by NMR-based metabonomics. This information is of critical importance when evaluating the comprehensive effect of cordycepin.

## 3. Materials and methods

### 3.1 Extraction and purification of cordycepin

The cultured fruiting body (1 kg) of *Cordyceps militaris* (L.) Link (provided by Hunan Yikang High-Tech Biology Co. Ltd., Huaihua, China) was soaked in EtOH overnight and extracted by thermal recycling extraction for 3–4 h (totally extracting for three times). The extract was concentrated under reduced pressure to dryness.

The residue was dissolved in alcohol, mixed with silica gel, evaporated to dryness, and baked for 3–4 h at 60°C. Cordycepin was separated by a GF254 SIL column (Φ 9 cm × 60 cm) with the mobile phase of petroleum ether/dichloromethane/methanol (1.5:3:0.6). Samples were collected (500 ml of each fraction) and traced by TLC, with the cordycepin reference substance (Sigma-Aldrich, Inc., Shanghai, China) as a control. The fraction with cordycepin was concentrated under reduced pressure to dryness and recrystallized with ethanol. Light yellow or white crystal was collected and identified as 3'-deoxyadenosine by spectral analysis (NMR, MS) and elemental analysis with a purity of ≥ 99% (HPLC).

### 3.2 Animal and diets

Twelve-month-old Syrian golden hamsters were obtained from Vital River Laboratory Animal Technology Co. Ltd., Beijing, China. All protocols in this study were in accordance with National Institutes of Health regulations for the care and use of animals in research. Throughout the
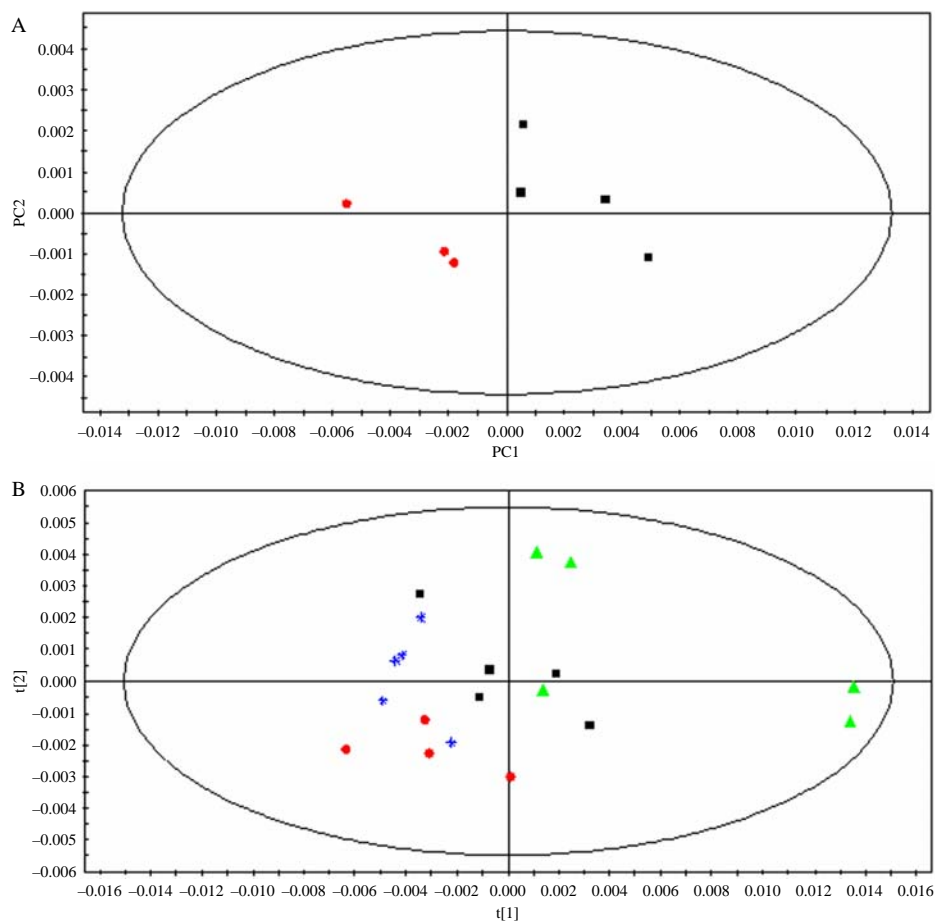
Figure 6. PR analysis of HR-MAS $^1$H NMR CPMG spectra of liver tissues from hamsters. (A): OPLS-DA analysis of the spectra of liver tissues from normal and hyperlipidemic hamsters. (B): Scores plot of OPLS-DA analysis of the spectra of liver tissues from the four groups of hamsters. ●, Control hamsters; ■, hyperlipidemic hamsters; ▲, hyperlipidemic hamsters treated with an simvastatin (2 mg kg$^{-1}$); and *, hyperlipidemic hamsters with an administration of cordycepin (140 mg kg$^{-1}$).

acclimatization and study periods, all animals had access to corresponding food and water *ad libitum* and were maintained on a 12 h light/dark cycle (21 ± 2°C with a relative humidity of 45 ± 10%).

Twenty adult male Syrian golden hamsters (90–110 g) were acclimatized for 7 days in cages prior to model construction. Then animals were randomly allocated into two groups, control ($n = 5$) and hyperlipidemic ($n = 15$). The hamsters that served as the reference group were fed the standard chow *ad libitum*, while the hyperlipidemic hamsters were

fed a HFD (Institute of Laboratory Animal Sciences, Beijing, China) per day for 2 weeks to establish hyperlipidemic model.

Two kinds of experimental diets and their ingredients were as follows:

A standard chow: 20% flour, 10% rice flour, 20% soybean meal, 20% corn, 25% wheat bran, 2% bone meal, and 2% fish meal.

A HFD: 79.8% standard diet, 20% fat, and 0.2% cholesterol.

The hyperlipidemic hamsters were divided into three groups with consideration to the levels of triglyceride and cholesterol

in serum, together with weight, which were model control group, simvastatin ($2\,mg\,kg^{-1}$) or cordycepin ($140\,mg\,kg^{-1}$) treated group ($n = 5$). The normal hamsters were administrated with 2.5% carboxymethyl cellulose sodium. The hyperlipidemic hamsters were treated with an oral administration of drug per day for consecutive 4 weeks.

Then hamsters were anesthetized with an intra-peritoneal injection of 2 ml of 3% sodium pentobarbital per kilogram. An abdominal incision was made to expose the liver and inferior vena cava. A total of 3–4 ml of blood was withdrawn from the abdominal aorta into tubes with heparin for collecting plasma. After blood collection, liver was excised and weighted. One set of liver tissue was immediately snap frozen wrapped in aluminum foil in liquid nitrogen.

### 3.3   Plasma and intact liver collection

Blood in heparinized tubes was centrifuged at $12,000g$ for 15 min and the supernatant (plasma) was collected. Both plasma and liver samples were stored at $-80°C$ for the measurement of $^1H$ NMR spectrum.

### 3.4   $^1H$ NMR spectroscopy

All NMR experiments were carried out on a Bruker AVANCE III-500 spectrometer (Bruker Biospin, Rheinstetten, Germany), operating at a $^1H$ frequency of 500.13 MHz. The 90° pulse length was adjusted individually for each sample. Plasma spectra were measured at 25°C by triple resonance inverse TXI [$^1H$, $^{13}C$, $^{15}N$]-xyz triple axis gradient probe, and data of intact liver samples were acquired at 4°C and at a spinning rate of 4 kHz. A total of 128 transients were collected into 32 k data points for each spectrum with a spectral width of 20 ppm and a recycle delay of 4.0 s.

Three kinds of $^1H$ NMR spectra were acquired for the samples, a standard one-dimensional pulse sequence, using the first increment of the NOESY pulse sequence to achieve water presaturation and a Carr-Purcell-Meiboom-Gill (CPMG) pulse sequence [17] to enhance the contribution of low-molecular-weight metabolites. In addition, to observe the lipid contents of lipoproteins in plasma, diffusion-edited experiments were also carried out with bipolar pulse pair longitudinal eddy current delay (BPP-LED) pulse sequence [17–19]. A line-broadening factor of 0.3–1 Hz was applied to FIDs before that the Fourier transformation.

### 3.4.1   $^1H$ NMR spectroscopy on plasma

Plasma (30 μl) was added into 60 μl of 0.9% saline ($D_2O:H_2O = 1:9$) containing 0.1% sodium 3(trimethylsilyl)propionate-2,2,3,3-d4 (TSP) (an internal standard, chemical shift δ 0.0) in Eppendorf tubes. Centrifuged at $12,000g$ for 5 min at 25°C, 60 μl of sample was transferred into 1.7 mm NMR tubes. 1D NOESY, CPMG, and BPP-LED spectra were measured.

### 3.4.2   HR-MAS $^1H$ NMR spectroscopy on intact liver

Frozen samples were taken from a $-80°C$ freezer and placed in a cry vial and in liquid $N_2$ until insertion into a 4 mm (o.d.) $ZrO_2$ rotor. The pre-cooled rotor was filled with cooled $D_2O$ with 0.1% TSP after sample insertion. Spherical inserts were used in all cases, limiting the rotor inner volume to 12 μl.

$^1H$ NMR spectra of liver were recorded using a standard 1D-NOESY and the CPMG pulse sequence.

### 3.5   Metabolite identification

Both visual inspection of the raw spectral data and statistical results were used to prioritize the identification of discriminating

peaks. The metabolites in plasma and liver were identified with reference to the published literature data [20,21] and using the Chenomx NMR Suite (Chenomx, Calgary, Canada).

### 3.6 Data reduction of NMR spectra and PR analysis

The acquired NMR spectra were referenced to the chemical shift of TSP. Following phase and baseline correction, the $^1$H NMR spectra were automatically reduced to ASCII files using AMIX (Analysis of MIXtures software v. 3.0, Bruker Biospin). Each spectral region was normalized to the total of all the resonance integral regions and reduced to 'buckets' of equal width (0.04 ppm) over the range of 0.5–6.0 ppm. The regions containing the resonance from residual water (4.7–5.1 ppm) were excluded. The generated ASCII files were imported into SIMCA-P12.0 (Umetrics, Umeå, Sweden) for the PR analysis. Prior to the analysis, the values of all variables were mean centered.

PCA was used for the reduction of the dimensionality of the data sets, for the overview of the data set and the spotting of outliers, and then for the detection of any grouping or separation trend.

Partial least square discrimination analysis (PLS-DA) is a frequently used PLS-based classification method to find the best possible discriminant function (model) that separates classes of observations based on their $X$ variables.

When group separation was not satisfied based on PLS-DA, the data were further preprocessed using orthogonal signal correction to eliminate the inter-subject variability and to describe maximum separation based on class [22].

### Acknowledgements

### References

[1] R.L. Pollex, T.R. Joy, and R.A. Hegele, *Expert Opin. Emerg. Drugs* **13**, 363 (2008).

[2] Y. Yun, S. Han, S. Lee, S.K. Ko, C. Lee, N. Ha, and K. Kim, *Nat. Prod. Sci.* **9**, 291 (2003).

[3] P. Guo, K. Qu, J. Gao, Z.Q. Lian, C.M. Wu, C.A. Wu, and H.B. Zhu, *J. Pharmacol. Sci.* **113**, 395 (2010).

[4] C.C. Susan, K.H. Michael, C. Adam, F.S. Randall, and E.R. Terence, *Mol. BioSyst.* **6**, 909 (2010).

[5] J.C. Lindon, E. Holmes, M.E. Bollard, E.G. Stanley, and J.K. Nicholson, *Biomarkers* **9**, 1 (2004).

[6] J.K. Nicholson, E. Holmes, J.C. Lindon, and I.D. Wilson, *Nat. Biotechnol.* **22**, 1268 (2004).

[7] G. Sinta, *Science* **310**, 965 (2005).

[8] M. Van Doorn, J. Vogels, A. Tas, E.J. Van Hoogdalem, J. Burggraaf, A. Cohen, and J. Van Der Greef, *Br. J. Clin. Pharmacol.* **63**, 562 (2007).

[9] J.C. Lindon, E. Holmes, and J.K. Nicholson, *Expert Rev. Mol. Diagn.* **4**, 189 (2004).

[10] B. Wilcken, V. Wiley, J. Hammond, and K. Carpenter, *N. Engl. J. Med.* **348**, 2304 (2003).

[11] K. Valeille, J. Ferezou, G. Amsler, A. Quignard-Boulange, M. Parquet, D. Gripois, V. Dorovska-Taran, and J.C. Martin, *Am. J. Physiol. Heart Circ. Physiol.* **289**, H652 (2005).

[12] K. Valeille, J. Ferezou, M. Parquet, G. Amsler, D. Gripois, A. Quignard-Boulange, and J.C. Martin, *J. Nutr.* **136**, 1305 (2006).

[13] I.F. Duarte, B.J. Goodfellow, A. Barros, J.G. Jones, C. Barosa, L. Diogo, P. Garcia, and A.M. Gil, *NMR Biomed.* **20**, 401 (2007).

[14] M. Liu, H. Tang, J.K. Nicholson, and J.C. Lindon, *Magn. Reson. Chem.* **40**, S83 (2002).

[15] W. Willker and D. Leibfritz, *Magn. Reson. Chem.* **36**, S79 (1998).

[16] H.C. Bertram, I.F. Duarte, A.M. Gil, K.E. Bach Knudsen, and H.N. Lærke, *Anal. Chem.* **79**, 168 (2007).

[17] O. Beckonert, H.C. Keun, T.M.D. Ebbels, J. Bundy, E. Holmes, J.C. Lindon, and J.K. Nicholson, *Nat. Protocols.* **2**, 2697 (2007).

[18] D. Wu, A. Chen, and C.S. Johnson, *J. Magn. Reson.* **115**, 260 (1995).

[19] B.M. Beckwith-Hall, N.A. Thompson, J.K. Nicholson, J.C. Lindon, and E. Holmes, *Analyst* **128**, 814 (2003).

[20] W.M.T. Fan, *Prog. Nucl. Magn. Reson. Spectrosc.* **28**, 161 (1996).

[21] M.E. Bollard, S. Garrod, E. Holmes, J.C. Lincoln, E. Humpfer, M. Spraul, and J.K. Nicholson, *Magn. Reson. Med.* **44**, 201 (2000).

[22] C.L. Gavaghan, I.D. Wilson, and J.K. Nicholson, *FEBS Lett.* **530**, 191 (2002).